Journal of Industrial and Engineering Chemistry 20 (2014) 426–434

Contents lists available at SciVerse ScienceDirect

Journal of Industrial and Engineering Chemistry

journal homepage: www.elsevier.com/locate/jiec

Open circuit voltage increase by substituted spacer and thieno[3,4-c]pyrrole-4,6-dione for polymer solar cells

Kwan Wook Song, Min hee Choi, Myung hee Han, Doo Kyung Moon *

Department of Materials Chemistry and Engineering, Konkuk University, 1 Hwayang-dong, Gwangjin-gu, Seoul 143-701, Republic of Korea

ARTICLE INFO

Article history:
Received 7 February 2013
Accepted 28 April 2013
Available online 4 May 2013

Keywords:
Organic photovoltaics (OPVs)
Thieno[3,4-c]pyrrole-4,6-dione(TPD)
Electron donating characteristic

ABSTRACT

We reported on two donor polymers containing thieno[3,4-c]pyrrole-4,6-dione(TPD) derivatives as electron withdrawing units for organic photovoltaics (OPVs). To control molecular weight and solubility of polymers, hexyl side chains are inserted to thiophene spacers. Due to the electron donating characteristic of hexyl side chains, highest occupied molecular orbital (HOMO) energy level of polymer is decreased as 0.18 eV, whereas the open circuit voltage is increased to 1.08 V. When bulk heterojunction devices were fabricated, the best PCE value of 0.360% (V_{OC} = 0.89 V, J_{SC} = 1.2 mA/cm^2, FF = 36.3%) under 100 mW/cm^2 irradiation.

© 2013 The Korean Society of Industrial and Engineering Chemistry. Published by Elsevier B.V. All rights reserved.

1. Introduction

Polymer semiconductors which consist of various aromatic rings have been vigorously studied for the past several decades. These polymer semiconductors were developed for organic electronics, such as organic photovoltaics (OPVs) [1–8], organic thin film transistors [9–11] and organic light emitting diodes (OLEDs) [12–15]. Particularly, OPVs have drawn great attention owing to their various advantages such as low cost, light weight and great flexibility. Recently, the potential of OPVs have been enhanced because of developments of materials with high-efficiency [16,17] and studies for enhanced photo and oxidation stability of π-conjugated polymers [18]. In addition, OPVs are applicable for solution process technology, such as ink-jet printing and roll-to-roll fabrication to realized flexible and large area devices. As a result, the feasibility of energy converting device of next generation would be increased [19–22].

The key technologies in developing high-efficiency OPVs are the design and synthesis of polymer semiconductor materials. To develop high-efficiency polymeric photovoltaic materials, many systems have been used. In particular, a donor–acceptor (D–A) polymer system is useful to adjust the band gaps of polymers by overlapping orbitals which is induced by intra-chain charge transfer [23,24]. In order to develop outstanding donor–acceptor (D–A) copolymers, it is important to consider the following properties: (1) good solubility in organic solvents, such as chlorobenzene and/or *o*-dichlorobenzene, (2) low band gap for board absorption area, (3) lowering the highest occupied molecular orbital (HOMO) energy levels to get high open-circuit voltage (V_{OC}) and (4) high charge carrier mobility [25]. The mentioned properties are critical factors which determine high oxidative stability and effective charge separation of D–A type polymers. Especially, it is required to introduce various alkyl chains in order to enhance solubility of D–A type polymers. For using this method, intermolecular interaction among polymers can be enhanced and the control of morphology could be possible. If D–A type polymers have a low HOMO level, in addition, good oxidative stability would be possible and high V_{OC} would be expected.

Thieno[3,4-c]pyrrole-4,6-dione (TPD) is one of electron-withdrawing materials which has a symmetrical, compact, rigidly fused and coplanar structure. Because various functional groups can be introduced to the pyrrole site, it is possible to control solubility, processability and energy level of synthesized polymer [26]. Thus, D–A type polymers containing TPD unit would enhance intra- and interchain interaction, form a quinoidal structure by a thiophene-maleinide structure and stabilize the excited state energy. As a result, TPD-based polymers would show a high V_{OC}. Recently, Leclerc et al. reported the polymer with benzo[1,2-b;3,4-b]dithiophene (BDT) as an electron-donating unit and TPD as an electron-withdrawing moiety. The polymer was confirmed 5.5% of PCE with −5.56 eV of the HOMO level and 0.85 V of V_{OC}. Also, Tao et al. reported polymer with 7.3% of PCE (HOMO level: −5.57 eV and V_{OC}: 0.88 V) by polymerizing dithienosilole and TPD unit [27]. And, Reynolds et al. reported the polymer with 7.3% of PCE by polymerizing with dithienogermole and TPD unit [28].

* Corresponding author. Tel.: +82 2 450 3498; fax: +82 2 444 0765.
E-mail address: dkmoon@konkuk.ac.kr (D.K. Moon).

1226-086X/$ – see front matter © 2013 The Korean Society of Industrial and Engineering Chemistry. Published by Elsevier B.V. All rights reserved.
http://dx.doi.org/10.1016/j.jiec.2013.04.037

In this study, two D–A type polymers were synthesized through Suzuki coupling reaction. Using TPD as an electron-withdrawing moiety, poly(9,9′-dioctylfluorene-*alt*-5,5′-di-thienyl-*N*-ethyl hexyl thieno[3,4-c]pyrrole-4,6-dione) and poly(9,9′-dioctylfluorene-*alt*-5,5′-di-3-hexylthiophen-yl-*N*-ethyl hexyl thieno[3,4-c]pyrrole-4,6-dione), namely PFTPD and PFTPD6, respectively, were synthesized. An alkyl chain was introduced to a spacer to control the solubility of the polymer. UV-absorption spectra and energy level of polymers were measured. Moreover, V_{OC} was showed through the fabrication of a bulk hetero-junction solar cells by using [6,6]-phenyl C_{71} butyric acid methyl ester ($PC_{71}BM$) as an acceptor.

2. Results and discussion

Scheme 1 shows the chemical structure and the synthetic routes. **4-(a)** and **4-(b)** were synthesized through Stille coupling reaction, followed by bromination with *N*-bromosuccinimide. To enhance the solubility and film-forming characteristics of the final polymers, 2-ethyl hexyl group of TPD and *n*-hexyl side chain of the thiophene were introduced. The alternating copolymers, PFTPD and PFTPD6, were synthesized through Suzuki coupling reaction by using monomer 4 and 5. Polymerizations were performed in a degassed mixture of toluene as a solvent, paladium catalyst(0), monomer 4 and 5. To the solution, degassed 2 M K_2CO_3 aqueous solution (3:2 in volume ratios) and Aliquat 336 (as a surfactant) were added. The mixture was vigorously stirred at 100 °C for 48 h under N_2 atmosphere. After polymerization, bromobenzene and phenyl boronic acid were added for end-capping the polymer. The synthesized polymers were purified through washing with methanol, acetone, and hexane in a Soxhlet apparatus for 24 h, respectively. The chloroform soluble fraction was re-precipitated in methanol. The yields of polymers were 23 and 59%, respectively.

All polymers were dissolved in general organic solvents such as THF, chloroform, chlorobenzene and *o*-dichlorobenzene. Table 1 shows the molecular weight and thermal properties of synthesized PFTPD and PFTPD6 polymers. The number average molecular weight (Mn) of PFTPD and PFTPD6 were 7.6 and 14.6 kg/mol and polydispersity indexes (PDI) were 1.35 and 1.96, respectively. Because of hexyl side chain, PFTPD6 showed enhanced degree of polymerization (DP) and good solubility rather than PFTPD [29]. To increase the molecular weight and degree of polymerization of PFTPD and PFTPD6, the lengths of side chain which introduced to fluorene and TPD would be extend instead of introducing side chain to the spacer. PFTPD and PFTPD6 showed high thermal stability around 268 and 261 °C of decomposition temperature (T_d) at 5 wt% loss.

Fig. 1 showed the UV–vis absorption spectra of PFTPD and PFTPD6 in a chloroform solution (a) and in solid state (b). The maximum absorption peaks (λ_{max}) of PFTPD and PFTPD6 were observed at 466 nm and 430 nm in solution, respectively. Also, The λ_{max} of PFTPD (468 nm) and PFTPD6 (441 nm) in solid state were slightly red-shifted by 2 nm and 11 nm from solution to film state, respectively. And, the optical band gaps of PFTPD and PFTPD6 were 2.16 and 2.28 eV which was calculated from the band edge on the film, 569 nm and 525 nm. The intermolecular interaction among polymer chains was weak in solid state [26]. Also, the intermolecular interaction was limited because of the bulky side chain introduced to the fluorene and TPD unit [30]. The molar absorption coefficient of PFTPD and PFTPD6 were 3.01×10^4 and $3.07 \times 10^4\ M^{-1}\ cm^{-1}$, respectively. They were calculated according to Lambert–Beer's law. The absorption range of PFTPD and PFTPD6 was not broadened compared to other D–A type copolymers containing benzothiadiazole moieties [26,31–35]. This is because TPD has weak electron-withdrawing characteristics compared to 2,1,3-benzothiadiazole (BT) [16].

To understand the electronic properties of PFTPD and PFTPD6, the molecular geometries and electron density of states were simulated using density functional theory (DFT). DFT was performed using Gaussian 09 for a hybrid B3LYP correlation functional and a split-valence 6-31G(d) basis set. As shown in Fig. 2

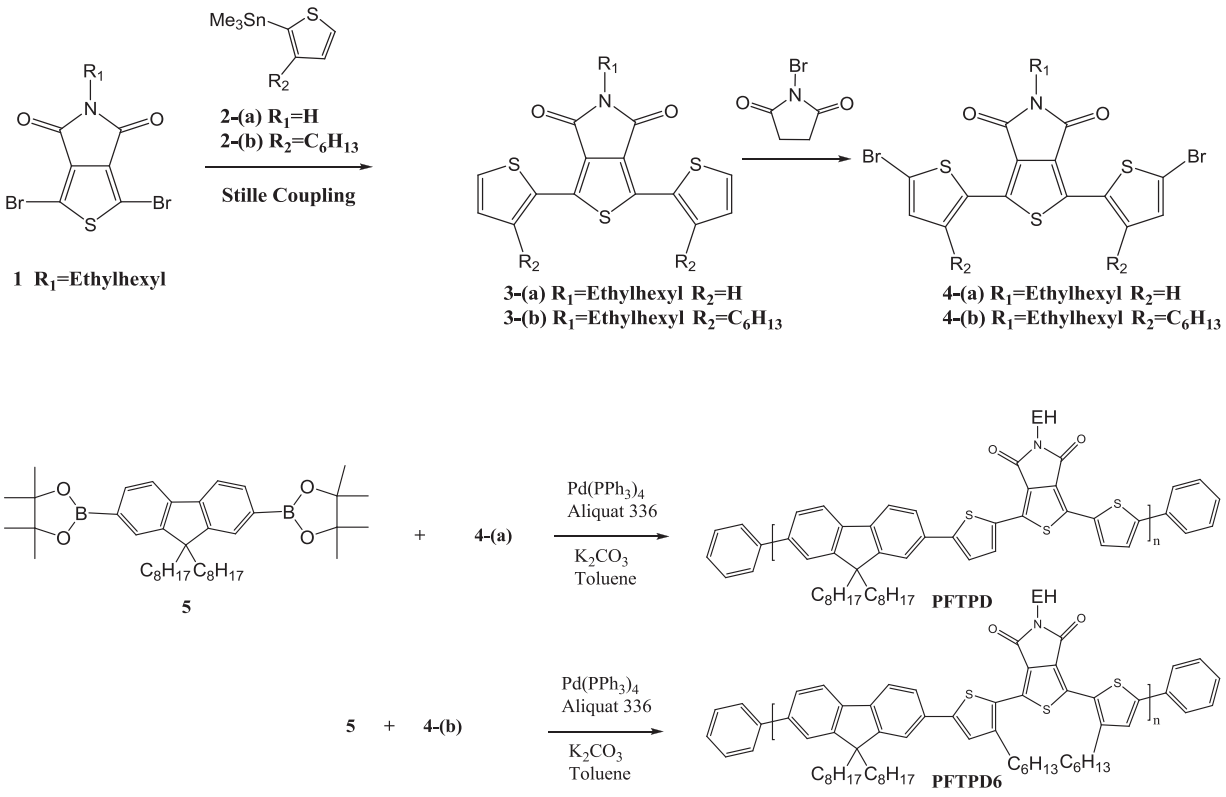

Scheme 1. The synthetic route of PFTPD and PFTPD6.

Table 1
Molecular weight and thermal properties of polymers.

Polymer	M_n (kg/mol)	M_w (kg/mol)	PDI	DP	T_d (°C)	Absorption λ_{max} (nm)[a]		ε ($\times 10^4$)	PL λ_{max} (nm)[b]		E_g^{OP} (eV)[c]
						Solution[d]	Film[e]		Solution[d]	Film[e]	
PFTPD	76	102	1.35	9	268	466	468	3.01	544	613	2.16
PFTPD6	146	287	1.96	15	261	430	441	3.07	534	584	2.28

[a] λ_{max} was determined from UV–vis data.
[b] λ_{max} was determined from PL data.
[c] Estimated from the onset of UV–vis absorption data of the thin film.
[d] Diluted in chloroform (10 μg/mL).
[e] Drop-casted from a chloroform.

and Table 2, the tilt angles and energy level of two polymer structure were showed. The tilt angles between thiophene spacer and TPD unit were increased to 43–45° in PFTPD6. Fig. 3 revealed the results of the DFT calculation in benzothiadiazole and TPD derivatives. When an alkyl chain was introduced to thiophene, in particular, the electron donating characteristic was enhanced. As a result, the HOMO level of TPD derivative decreased whereas the LUMO level increased, as shown in Fig. 3(a). This tendency was also found in PFTPD6. According to the calculated results in Fig. 3(b), fluorene unit showed the lowest HOMO level and confirmed a large band gap. In general, the band gap energy of a D–A type copolymer is reduced by the overlap of orbital that occurs by charge transfer between the electron-donating unit and electron-withdrawing unit [36]. Therefore, the band gap of polymer would be reduced if a strong electron-withdrawing unit was introduced to the polymer backbone. As a result of calculations, an effective intramolecular charge transfer might not be occurred because TPD had weaker electron affinity property, compared to 2,1,3-benzothiadiazole. However, it would be influential in lowering the HOMO level in polymers, because the HOMO levels of both TPD and fluorene were low. And, it would have a significant effect on an increase in oxidative stability and V_{OC} [37].

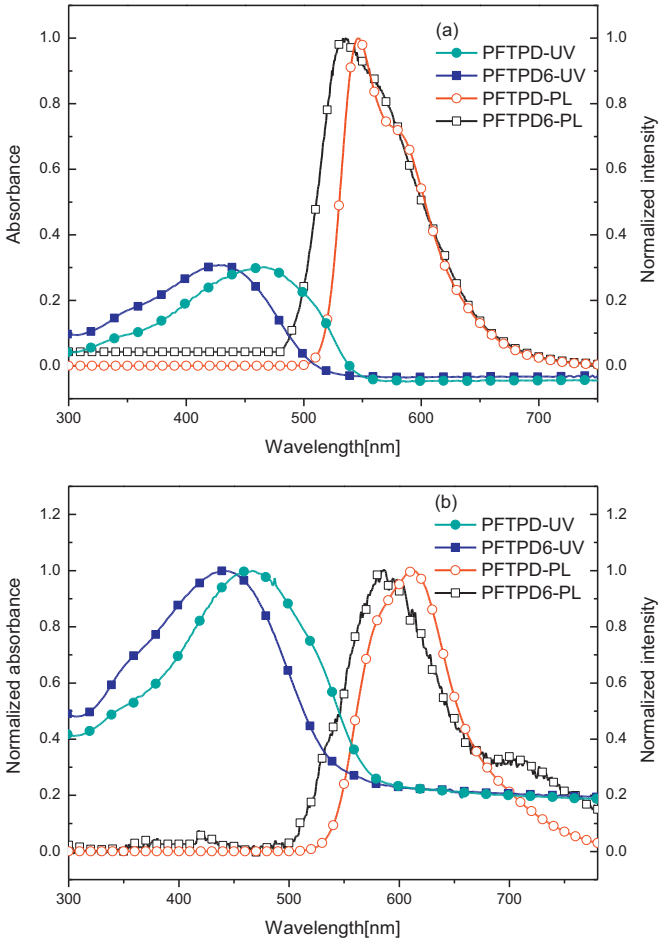

Fig. 1. UV–vis and photoluminescence spectrum of polymers (a) solution state in $CHCl_3$ at a concentration of 10 μg/mL; (b) film.

As shown in Fig. 4, the results of cyclic voltammetry (CV) were matched with the DFT calibration. The electrochemical behavior of the copolymers was investigated with CV. The electrolyte was 0.1 M tetrabutyl ammonium hexafluorophosphate (Bu_4NPF_6) in acetonitrile, and the scan rate of measurement was 100 mV/s. The ITO glass and Pt plates were used as the working and counter electrodes, respectively, and silver/silver chloride was used as the reference electrode. All of other measurements were calibrated using the ferrocene (HOMO level = −4.8 eV) as the standard. The HOMO levels of the polymers were determined using the oxidation onset (E_{ox}^{onset}). The electrochemical oxidation onsets of PFTPD and PFTPD6 were 1.03 and 1.27 V and the HOMO energy levels were calculated to 5.36 and 5.60 eV, respectively, which means good oxidative stability [38]. The HOMO level of PFTPD6 was lower than that of PFTPD due to the side chain introduced to a thiophene spacer. The side chain would play a role of decreasing the HOMO level of polymer. The LUMO energy levels were calculated from the difference between the HOMO energy levels and the optical band gap energies. According to the calculations, the LUMO energy levels of PFTPD and PFTPD6 were 3.19 and 3.30 eV, respectively. These LUMO energy levels were too high to apply the bulk heterojunction (BHJ) photovoltaic device. This means that strong electron-withdrawing characteristics are not found in TPD when fluorene is introduced as a donor. PFTPD and PFTPD6 would show high V_{OC} because it is determined based on the difference between the HOMO level of the donor and the LUMO level of the acceptor in the organic photovoltaic devices [39].

Bulk heterojunction solar cells using PFTPD and PFTPD6 as donor materials and $PC_{71}BM$ as an acceptor material were fabricated with a structure of ITO/PEDOT:PSS/polymer:$PC_{71}BM$/BaF_2/Ba/Al. Since UV–vis absorption property of $PC_{71}BM$ has a stronger than that of $PC_{61}BM$ in the visible region, especially around 500 nm. For this reason, $PC_{71}BM$ was used as an acceptor in this study [40,41]. All the photovoltaic measurements were performed under 100 mW/cm^2 AM 1.5 sun illumination in ambient conditions. Fig. 5 showed the *J–V* characteristic and incident photon-to-charge carrier efficiency (IPCE) of PSCs fabricated with PFTPD and PFTPD6. Also, the results of all photovoltaic performances are summarized in Table 3. The photovoltaic devices fabricated by PFTPD6 were optimized according to $PC_{71}BM$ ratio and annealing temperatures. As $PC_{71}BM$ ratio and annealing temperatures were increased, J_{SC} and FF were increased whereas V_{OC} was decreased. As expected in the HOMO energy level from the DFT and CV results in Figs. 3 and 4, high V_{OC} was observed in both

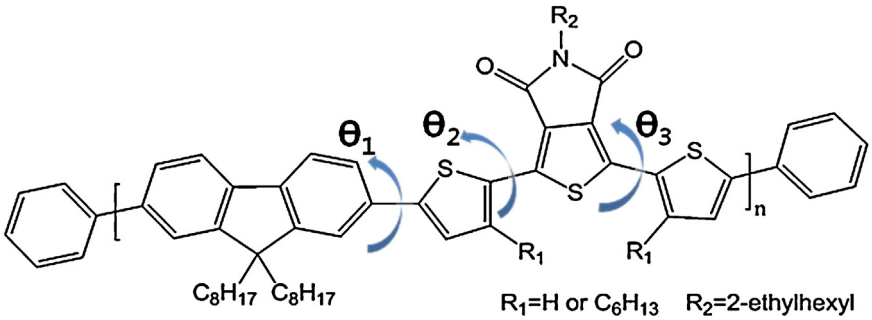

Fig. 2. Dihedral angles of polymers.

polymers. In PFTPD6, in particular, V_{OC} reached 1.08 V depending on PCBM ratio. However, J_{SC} and FF were limited in both polymers. As the results of device fabrication, PFTPD was showed a PCE of 0.360% (V_{OC} = 0.89 V, J_{SC} = 1.20 mA/cm^2, FF = 36.3%) and PFTPD6 was revealed a PCE of 0.11% (V_{OC} = 0.88 V, J_{SC} = 0.5 mA/cm^2, FF = 26.3%). The reduced J_{SC} and FF were confirmed due to the side chain which would promote steric hindrance.

The morphology of the polymer/$PC_{71}BM$ blend films was obtained using AFM on non-contact mode, as shown in Fig. 6. In both heterojunction thin films, it was unable to form a p-n channel. Instead, polymers were aggregated into a white spot. The route mean square (RMS) roughness of PFTPD6 was 5.28 nm, which is greater than that of PFTPD (0.67 nm). Thus, irregularity occurred from side chain might reduce J_{SC} because of hindering electron-hole separation and promoting electron–hole recombination.

3. Experiment

3.1. Materials

All starting materials were purchased from Sigma–Aldrich and Alfar Aesar, and used without further purification. Toluene and tetrahydrofuran (THF) were distilled from benzophenone and sodium. Other reagents and chemicals were used as received. 9,9-dioctyl-2,7-dibromofluorene was consumed after purifying by recrystallization. 5-(Octyl)thieno[3,4-c]pyrrole-4,6-dione, 2,2′-(9,9-dioctyl-9H-fluorene-2,7-diyl)bis(4,4,5,5-tetramethyl-1,3,2-dioxaborolane) were prepared as described in the literatures.

3.2. Synthesis

3.2.1. 1,3-Dibromo-(2-ethylhexyl)-5H-thieno[3,4-c]pyrrole-4,6-dione (**1**)

5-(2-Ethylhexyl)-5H-thieno[3,4-c]pyrrole-4,6-dione (2.0 g, 7.537 mmol) was dissolved in a mixture of sulfuric acid (11.5 mL) and trifluoroacetic acid (112 mL). While stirring, NBS (4.047 g, 22.61 mmol) was added in five portions to the solution and the reaction mixture was stirred at room temperature overnight. The brown-red solution was diluted with water (100 mL). The mixture was extracted with dichloromethane. The organic phase was dried over anhydrous sodium sulfate and the solvent was evaporated under reduced pressure. The crude product was purified by column chromatography using dichloromethane/hexanes (1:1 ratio) to afford 2.5 g of the title product as white needles (Y = 78%). ^{1}H NMR (400 MHz, $CDCl_3$, δ): 3.49 (d, 2H); 1.8 (m, 1H); 1.34–1.27 (m, 8H); 0.89 (t, 6H, J = 7.1 Hz).

3.2.2. 2-Bromo-3-hexylthiophene (**2-(b)-1**)

2-Bromo-3-hexylthiophene was synthesized below. First, 51.7 mL of acetic acid and 51.7 mL of $CHCl_3$ were added to a dry round bottom flask, and the flask was purged with nitrogen for 10 min. Then 3-hexylthiophene (8.7 g, 51.7 mmol) was added. The mixture was cooled to 5 °C, and NBS (9.2 g, 51.7 mmol) was added over a period of 1 h while the temperature was maintained at 5–10 °C. The mixture was stirred overnight and cooled in an ice bath. Then a dilute HCl solution (100 mL) was added, and the mixture was extracted with $CHCl_3$. The $CHCl_3$ layer was washed with water several times until a pH 6 was reached, and then this layer was dried over anhydrous Na_2SO_4. The solvent was removed through rotary evaporation. The residue was purified by column chromatography on a silica gel using hexane as the eluent. 2-Bromo-3-hexylthiophene (12 g, 50 mmol) was dissolved in THF (41 mL), and the solution was cooled to −78 °C. Then a 2.5 M solution of *n*-BuLi in THF (28 mL, 56 mmol) was added dropwise for 1 h. After stirring for 1 h at −78 °C, a 1.0 M solution of Me_3SnCl in THF (56 mL, 56 mmol) was added dropwise, and the mixture was stirred at −50 °C for 2 h. Then the solution was allowed to warm up to room temperature and was stirred 24 h. After the reaction was completed, the reaction mixture was poured into water and extracted with ether. The organic phase was washed with brine several times and dried over Na_2SO_4. The solvents were removed through rotary evaporation to afford a brown liquid. The residue was distilled under the reduced pressure to produce a 76% yield (15.6 g) of the product as a color-less oil. ^{1}H NMR (400 MHz, $CDCl_3$, δ): 6.85 (s, 1H); 2.55 (t, J = 7.6 Hz, 2H); 1.56 (t, J = 7.2 Hz, 2H); 1.31 (m, 6H); 0.88 (t, J = 6.8 Hz, 3H); 0.36 (t, J = 27.6 Hz, 9H).

3.2.3. 5. 5-(2-Ethylhexyl)-1,3-bis(3-hexylthiophen-2-yl)-4H-thieno[3,4-c]pyrrole-4,6(5H)-dione (**3-(a)**)

Compound **1** (1.0 g, 2.363 mmol) was dissolved into anhydrous THF (95 mL). 2-(tributylstannyl)thiophene (2.64 g,7.090 mmol), and bis(triphenylphosphine) palladium(II) dichloride (10 mg, 6%)

Table 2
Calculated dihedral angle and HOMO and LUMO energy levels.

	θ_1 (°)	θ_2 (°)	θ_3 (°)	E^{OX} (v)	E^{ON} (V)[a]	HOMO (eV)[b]	LUMO (eV)[c]
PFTPD	22.9	1.21	2.27	1.47	1.03	−5.36	−3.19
PFTPD6	26	44.9	43.6	1.54	1.27	−5.60	−3.30

[a]Onset oxidation potential
[b]Calculated from the reduction and oxidation potentials under the assumption that the absolute energy level of Fc/Fc$^+$ was 4.8 eV below a vacuum.
[c]Difference between optical bandgap and HOMO level calculated from b.

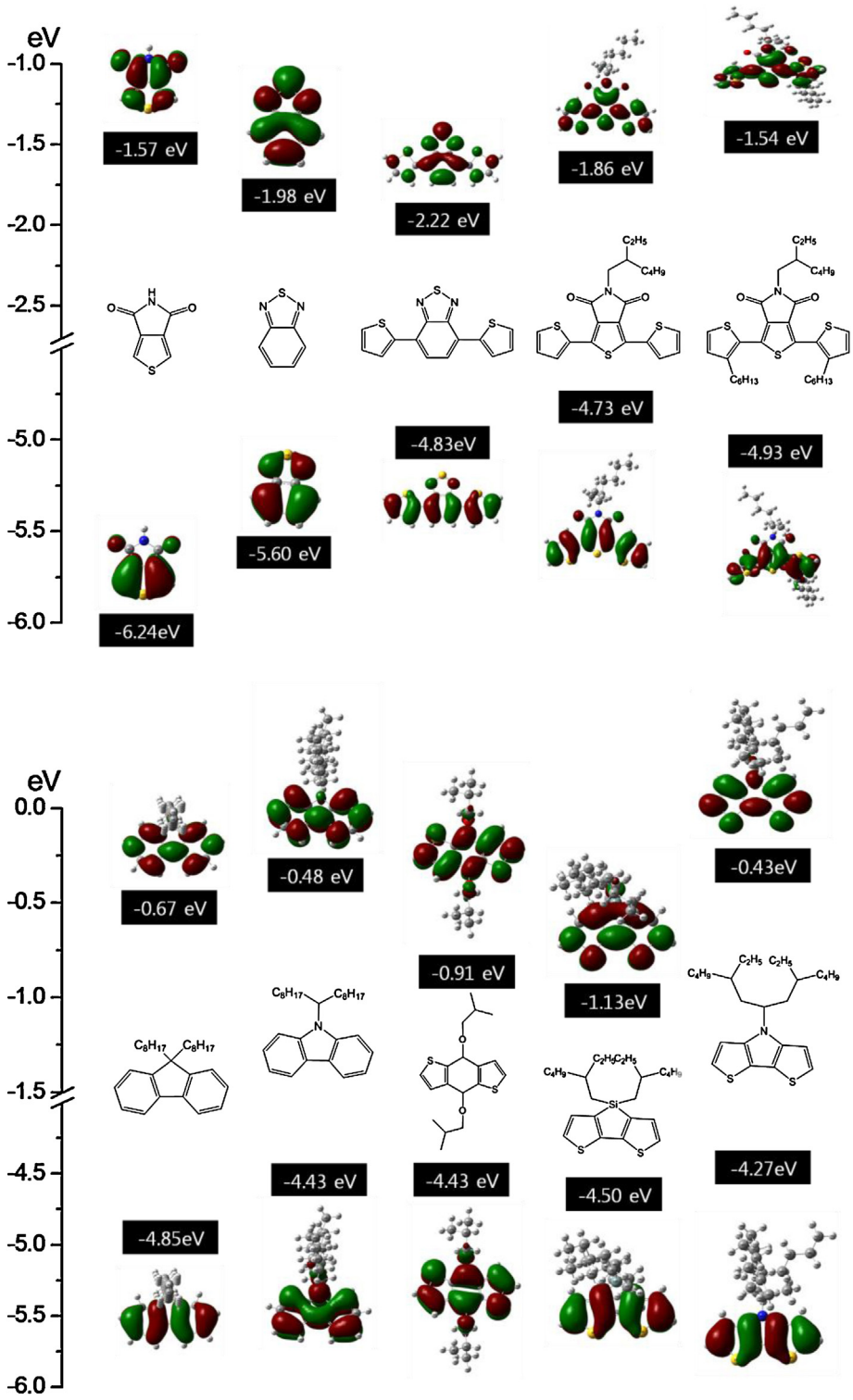

Fig. 3. Comparison of theoretical HOMO and LUMO energy levels (a) TPD, BT acceptor unit (b) general donor unit.

were added to the reaction mixture. The solution was refluxed for 24 h, then cooled and poured into water. The mixture was extracted twice with dichloromethane. The organic phases were combined, washed with brine, and dried over anhydrous sodium sulfate. The solvent was removed under reduce pressure and the crude product was purified by column chromatography using dichloromethane:hexanes as the eluent (ratio 1:1) to afford 1 g of the product as a green powder (Y = 98%). ^{1}H NMR (400 MHz, $CDCl_3$, δ): 8.33 (d, 2H); 7.78 (d, 2H); 7.34 (t, 2H, J = 4.2 Hz); 3.83 (t, 2H, J = 7.1 Hz); 1.89 (m, 2H); 1.53–1.47 (m, 10H); 1.05 (t, 3H, J = 7.2 Hz).

*3.2.4. 5-(2-Ethylhexyl)-1,3-bis(3-hexylthiophen-2-yl)-4H-thieno[3,4-c]pyrrole-4,6(5H)-dione (**3-(b)**)*

Compound **1-(b)** (1.5 g, 3.545 mmol) was dissolved into anhydrous THF (143 mL). 2-(trimethylstannyl-3-hexyl)thiophene (3.52 g,10.63 mmol), and bis(triphenylphosphine) palladium(II) dichloride (149 mg, 6%) were added to the reaction mixture. The

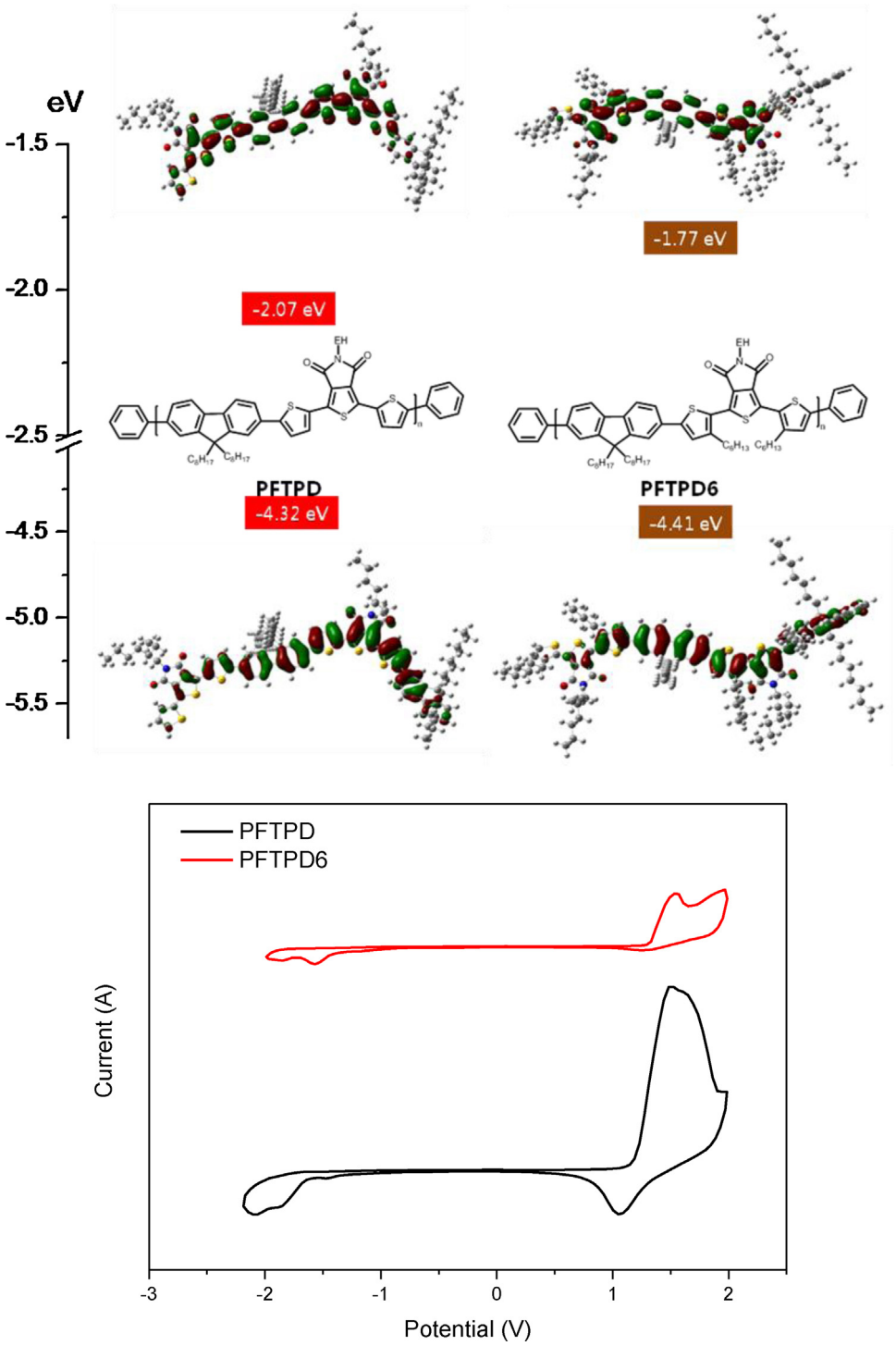

Fig. 4. Theoretical and measured energy level of PFTPD and PFTPD6.

solution was refluxed for 24 h then cooled and poured into water. The mixture was extracted twice with chloroform. The organic phases were combined, washed with brine, and dried over anhydrous sodium sulfate. The solvent was removed under reduce pressure and the crude product was purified by column chromatography using dichloromethane:hexanes as the eluent (ratio 1:1) to afford 1.6 g of the product as red sticky solid. (Y = 75%) [9]. ^{1}H NMR (400 MHz, $CDCl_3$, δ): 7.42 (d, 2H, *J* = 5.2 Hz); 7.02 (d, 2H, *J* = 5.2 Hz); 3.63 (t, 2H, *J* = 7.2 Hz); 1.78 (m, 1H, *J* = 7.9 Hz); 1.66–1.63 (m, 9H); 1.30–1.25(m, 26H); 0.88 (t, 6H, *J* = 6.4 Hz).

*3.2.5. 1,3-Di(2′-bromothien-5′-yl)-5-octylthieno[3,4-c]pyrrole-4,6-dione (**4-(a)**)*

This compound was synthesized as described for 2.3.9. using **3-(a)** (1.29 g, 3.00 mmol), a mixture of acetic acid and chloroform (60 mL) (ratio 1:1) at 0 °C, and *N*-bromosuccinimide (1.20 g, 6.67 mmol). The crude product was purified by gradient column chromatography using hexanes to dichloromethane:hexanes (ratio 1:1–2:3) to afford 1.72 g of the product as a bright yellow solid (*Y* = 98%). ^{1}H NMR (400 MHz, $CDCl_3$, *δ*): 7.65 (d, 2H, *J* = 4.0 Hz); 7.07 (d, 2H, *J* = 4.0 Hz); 3.54 (d, 2H, *J* = 7.3 Hz); 1.82 (t, 1H, *J* = 6.0 Hz); 1.38–1.29 (m, 8H); 0.92 (t, 6H, *J* = 2.9 Hz).

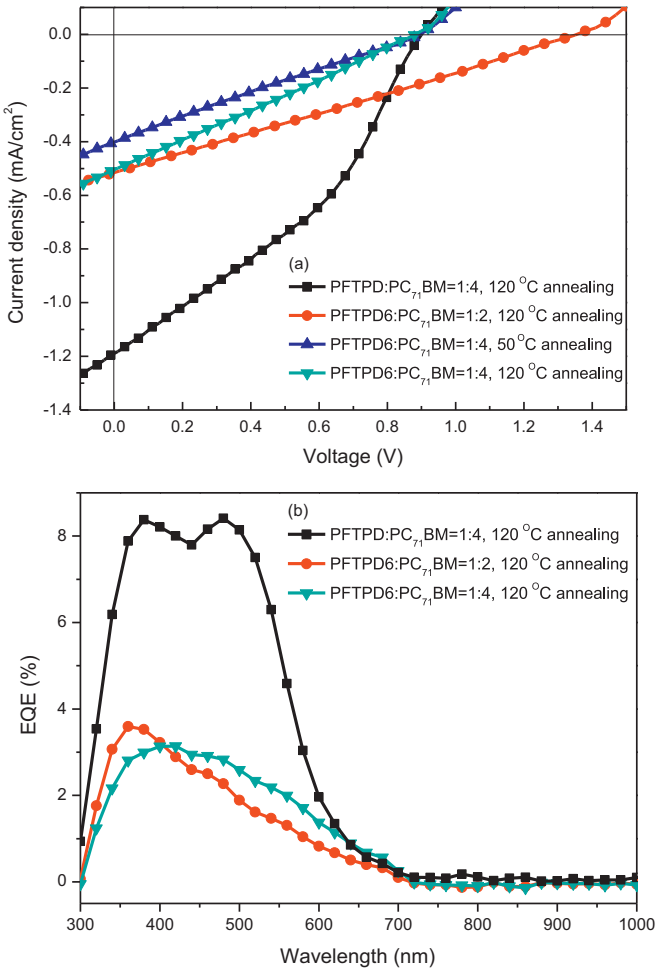

Fig. 5. (a) The *J–V* characteristics and (b) the IPCE spectra of BHJ solar cells with the device.

*3.2.6. 1,3-Bis(5-bromo-3-hexylthiophen-2-yl)-5-(2-ethylhexyl)-4H-thieno[3,4-c]pyrrole-4,6(5H)-dione (**4-(b)**)*

This compound was synthesized by using compound **3-(b)** (1.67 g, 2.793 mmol), a mixture of acetic acid and chloroform (93 mL) (ratio 1:1) at 0 °C, and *N*-bromosuccinimide (1.494 g, 8.379 mmol). After the addition of NBS, the cooling bath was removed and the reaction was stirred at ambient temperature for 24 h. The solution was then heated up to 55 °C for 24 h. The reaction was carefully monitored by thin layer chromatography (TLC). The reaction mixture was cooled and poured into water. The mixture was extracted several times using chloroform. The chloroform parts were combined, washed with brine, and dried over anhydrous sodium sulfate. The crude product was purified by column chromatography using dichloromethane:hexanes as the eluent (ratio 1:1) to afford 2 g of the product as a yellow solid (Y = 94%) ^{1}H NMR (400 MHz, $CDCl_3$, δ): 6.97 (s, 2H, J = 5.2 Hz); 3.51 (d, 2H, J = 7.2 Hz); 1.79 (m, 1H, J = 7.9 Hz); 1.66–1.63 (m, 9H); 1.30–1.25(m, 26H); 0.88 (t, 6H, J = 6.4 Hz).

3.3. Polymerization through the Suzuki coupling reaction

3.3.1. Poly[9,9-dioctyl-9H-fluorene-alt-1,3-di(2′-thien-5′-yl)-5-(2-ethylhexyl)-thieno[3,4–]pyrrole-4,6-dione] (PFTPD)

To a mixture of tetrakis(triphenyl-phosphine) Pd(0) (12 mg, 0.010 mmol, 2 mol%), 2,2′-(9,9-dioctyl-9H-fluorene-2,7-diyl)-bis(4,4,5,5-tetramethyl-1,3,2-dioxaaborolane) (compound **5**) (0.328 g, 0.510 mmol), and compound **4-(a)** (0.3 g, 0.510 mmol) was added a degassed mixture of toluene (|monomer| = 0.06 M) and 2 M K_2CO_3 aqueous solution (3:2 in volume). The mixture was vigorously stirred at 85–90 °C for 48 h under the nitrogen. After the mixture was cooled to room temperature, it was poured into the methanol. A powder was obtained by filtration was reprecipitated with methanol several times. The polymer was further purified by washing methanol and acetone, respectively, in a Soxhlet apparatus for 24 h and dried under reduced pressure at 50 °C. Red solid 0.1 g (23%) ^{1}H NMR (400 MHz, $CDCl_3$, δ): 7.70–7.52 (m, 5H), 3.59 (s, 1H), 2.03–2.01 (m, 10H), 1.58–0.83 (m, 69H).

3.3.2. Poly[9,9-dioctyl-9H-fluorene-alt-1,3-di-5′-(3-hexylthien-2′-yl)-5-(2-ethylhexyl)-thieno[3,4-c]pyrrole-4,6-dione] (PFTPD6)

PFTPD6 was polymerized through the same procedures with the compounds **5** and **4-(b)** instead of **4-(a)**. Brown solid of 0.12 g (59%) ^{1}H NMR (400 MHz, $CDCl_3$, δ): 7.69–7.48 (m, 7H), 7.41–7.33 (d, 4H), 3.61 (s, 1H), 2.87 (s, 1H), 2.72–0.65 (m, 73H).

3.4. Measurements

The ^{1}H NMR (400 MHz) spectra were recorded using a Brüker AMX400 spectrometer in $CDCl_3$, and the chemical shifts were recorded in units of ppm with TMS as the internal standard. The absorption spectra were recorded using an Agilent 8453 UV–vis spectroscopy system. The solutions that were used for the UV–vis spectroscopy measurements were dissolved in chloroform at a concentration of 10 μg/mL. The films were drop-coated from the chloroform solution onto a quartz substrate. All of the GPC analyses were carried out using THF as the eluent and a polystyrene standard as the reference. The TGA measurements were performed using a TG 209 F3 thermogravimetric analyzer. The cyclic voltammetric waves were produced using a Zahner IM6eX electrochemical workstation with a 0.1 M acetonitrile (substituted with nitrogen for 20 min) solution containing tetrabutylammonium hexafluorophosphate (Bu_4NPF_6) as the electrolyte at a constant scan rate of 50 mV/s. ITO, a Pt wire, and silver/silver chloride [Ag in 0.1 M KCl] were used as the working, counter, and reference electrodes, respectively. The electrochemical potential was calibrated against Fc/Fc^+. The HOMO levels of the polymers were determined using the oxidation onset value. Onset potentials are values obtained from the intersection of the two tangents drawn at the rising current and the baseline changing current of the CV curves. The LUMO levels were calculated from the differences between the HOMO energy levels and the optical

Table 3
Photovoltaic performances of polymers.

Active layer (w/w)		Weight ratio (P:A, w/w)	Pre-annealing (°)	V_{OC} (V)	J_{SC} (mA/cm^2)	FF (%)	PCE (%)
Polymer (P)	Acceptor (A)						
PFTPD	$PC_{71}BM$	1:4	120	0.89	1.2	36.3	0.36
PFTPD6	$PC_{71}BM$	1:2	120	1.08	0.14	20.5	0.03
		1:4	50	0.9	0.4	24.1	0.09
			120	0.88	0.5	26.3	0.11

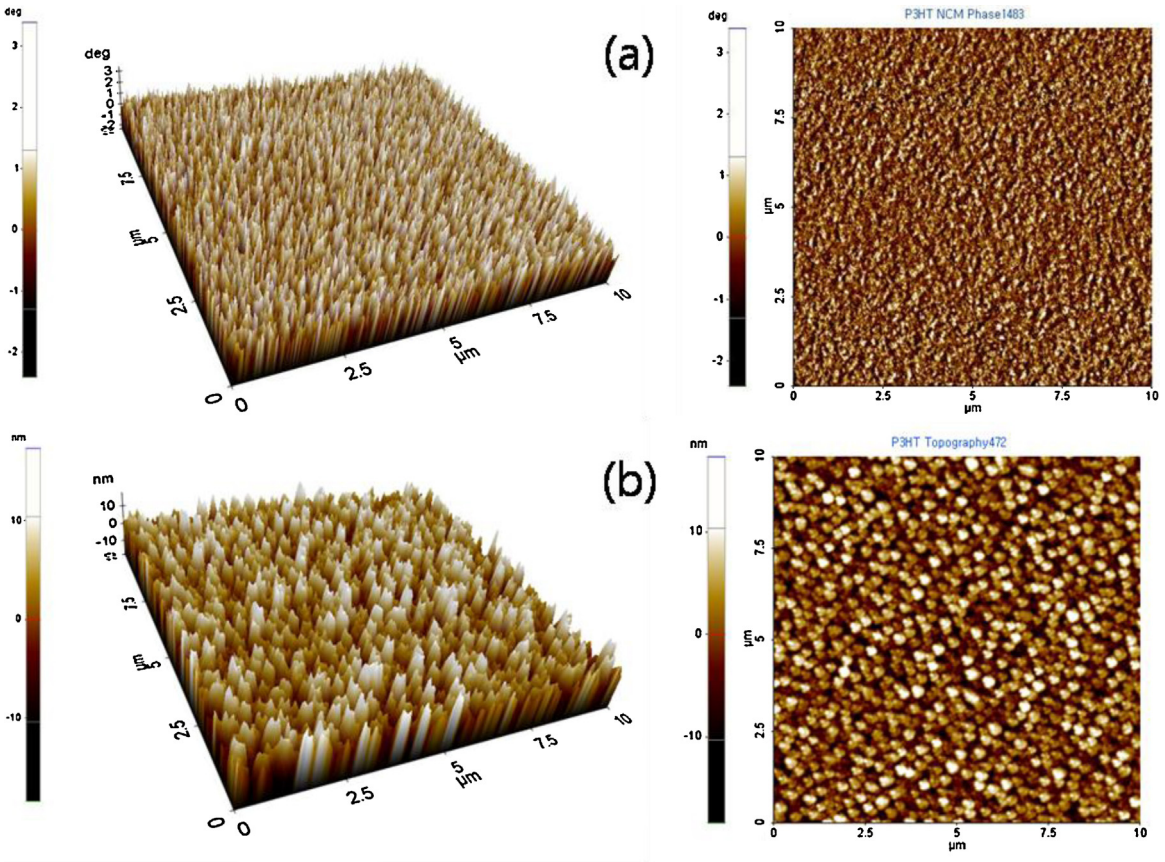

Fig. 6. AFM images of PFTPD (a) and PFTPD6 (b) measured by non-contact mode.

band-gaps, which were determined using the UV–vis absorption onset values in the films. The current density–voltage (*J*–*V*) curves of the photovoltaic devices were measured using a computer-controlled Keithley 2400 source measurement unit (SMU) that was equipped with a Class A Oriel solar simulator under an illumination of AM 1.5G (100 mW/cm^2). Topographic images of the active layers were obtained through atomic force microscopy (AFM) in tapping mode under ambient conditions using an XE-100 instrument.

3.5. Device fabrication and characterization

All of the bulk heterojunction PV cells were prepared using the following device fabrication procedure. The glass/indiumtinoxide (ITO) substrates [Corning, Korea (10 Ω/□)] were sequentially lithographically patterned, cleaned with detergent, and ultrasonicated in deionizedwater, acetone and isopropyl alcohol. Then the substrates were dried on a hot-plate at 120 °C for 10 min and treated with oxygen plasma for 10 min in order to improve the contact angle just before the film coating process. Poly(3,4-ethylene-dioxythiophene): poly(styrene-sulfonate) (PEDOT:PSS, BaytronP 4083 BayerAG) was passed through a 0.45 μm filter before being deposited on to ITO at a thickness of ca.32 nm by spin-coating at 4000 rpm and was dried at 120 °C for 20 min inside a glovebox. Composite solutions with polymers and PCBM were prepared using 1,2-dichlorobenzene (o-DCB). The concentration was controlled adequately in the 1.0 wt% range, and the solutions were then filtered through a 0.45 mm PTFE filter and then spin-coated on top of the PEDOT:PSS layer. The device fabrication was completed by depositing thin layers of BaF_2 (1 nm), Ba (2 nm) and Al (200 nm) at pressures of less than 10^{-6} torr. The active area of the device was 4 mm^2. Finally, the cell was encapsulated using UV-curing glue (Nagase, Japan). In this study, all of the devices were fabricated with the following structure: ITO glass/PEDOT:PSS/polymer:$PC_{71}BM$/BaF_2/Ba/Al. The illumination intensity was calibrated using a standard Si photodiode detector that was equipped with a KG-5filter. The output photocurrent was adjusted match the photocurrent of the Si reference cell in order to obtain a power density of 100 mW/cm^2. After the encapsulation, all of the devices were operated under an ambient atmosphere at 25 °C.

4. Conclusions

In this study, two polymers, PFTPD and PFTPD6, were polymerized by introducing TPD as the electron-withdrawing unit of a donor–acceptor type polymer. By introducing a side chain to the spacer, the degree of polymerization and the band gap of polymer were increased. The band gaps of PFTPD and PFTPD6 were 2.16 and 2.28 eV. Also, in PFTPD6, the HOMO energy level was lowered whereas the LUMO energy level was increased. Because of low HOMO levels, relatively high V_{OC} was observed in PFTPD6. When a solar cell was fabricated with $PC_{71}BM$ as an acceptor, the PFTPD was showed a PCE of 0.36%. (V_{OC} = 0.89 V, J_{SC} = 1.20 mA/cm^2 and FF = 36.3%).

Conflict of interest

The authors declare no competing financial interest.

Acknowledgments

This research was supported by a grant from the Fundamental R&D Program for Core Technology of Materials funded by the Ministry of Knowledge Economy, Republic of Korea. This work was supported by the National Research Foundation of Korea Grant

funded by the Korean Government (MEST) (NRF-2009-C1AAA001-2009-0093526).

References

[1] H. Bronstein, Z. Chen, R.S. Ashraf, W. Zhang, J. Du, J.R. Durrant, P.S. Tuladhar, K. Song, S.E. Watkins, Y. Geerts, M.M. Wienk, R.A.J. Janssen, T. Anthopoulos, H. Sirringhaus, M. Heeney, I. McCulloch, Journal of the American Chemical Society 133 (2011) 3272.
[2] K.H. Ong, S.L. Lim, H.S. Tan, H.K. Wong, J. Li, Z. Ma, L.C.H. Moh, S.H. Lim, J.C. de Mello, Z.K. Chen, Advanced Materials 23 (2011) 1409.
[3] G. Zhao, Y. He, C. He, H. Fan, Y. Zhao, Y. Li, Solar Energy Materials and Solar Cells 95 (2011) 704.
[4] M. Manceau, E. Bundgaard, J.E. Carlé, O. Hagemann, M. Helgesen, R. Søndergaard, M. Jørgensen, F.C. Krebs, Journal of Materials Chemistry 21 (2011) 4132.
[5] L. Huo, J. Hou, S. Zhang, H.Y. Chen, Y. Yang, Angewandte Chemie International Edition 49 (2010) 1500.
[6] Y. Zou, A. Najari, P. Berrouard, S. Beaupré, B.R. Aïch, Y. Tao, M. Leclerc, Journal of the American Chemical Society 132 (2010) 5330.
[7] R.S. Ashraf, J. Gilot, R.A.J. Janssen, Solar Energy Materials and Solar Cells 94 (2010) 1759.
[8] J.Y. Lee, W.S. Shin, J.R. Haw, D.K. Moon, Journal of Materials Chemistry 19 (2009) 4938.
[9] Y. Li, P. Sonar, S.P. Singh, M.S. Soh, M. vanMeurs, J. Tan, Journal of the American Chemical Society 133 (2011) 2198.
[10] P.M. Beaujuge, W. Pisula, H.N. Tsao, S. Ellinger, K. Müllen, J.R. Reynolds, Journal of the American Chemical Society 131 (2009) 7514.
[11] B.S. Ong, Y. Wu, Y. Li, P. Liu, H. Pan, Chemistry: A European Journal 14 (2008) 4766.
[12] J. Wang, C. Zhang, C. Zhong, S. Hu, X. Chang, Y. Mo, X. Chen, H. Wu, Macromolecules 44 (2011) 17.
[13] J.Y. Lee, M.H. Choi, D.K. Moon, J.R. Haw, Journal of Industrial and Engineering Chemistry 16 (2010) 395.
[14] K.S. Yook, J.Y. Lee, Journal of Industrial and Engineering Chemistry 16 (2010) 230.
[15] S.O. Kim, H.C. Jung, M.J. Lee, C. Jun, Y.H. Kim, S.K. Kwon, Journal of Polymer Science Part A: Polymer Chemistry 47 (2009) 5908.
[16] Z.-G. Zhang, J. Wang, Journal of Materials Chemistry 22 (2012) 4178.
[17] L. Huo, L. Ye, Y. Wu, Z. Li, X. Guo, M. Zhang, S. Zhang, J. Hou, Macromolecules 45 (2012) 6923.
[18] M. Jørgensen, K. Norrman, F.C. Krebs, Solar Energy Materials and Solar Cells 92 (2008) 686.
[19] F.C. Krebs, J. Fyenbo, M. Jørgensen, Journal of Materials Chemistry 20 (2010) 8994.
[20] F.C. Krebs, T. Tromholt, M. Jørgensen, Nanoscale 2 (2010) 873.
[21] F.C. Krebs, T.D. Nielsen, J. Fyenbo, M. Wadstrøm, M.S. Pedersen, Energy and Environmental Science 3 (2010) 512.
[22] F.C. Krebs, Solar Energy Materials and Solar Cells 93 (2009) 465.
[23] R. Kroon, M. Lenes, J.C. Hummelen, P.W.M. Blom, B. de Boer, Polymer Reviews 48 (2008) 531.
[24] E. Bundgaard, F.C. Krebs, Solar Energy Materials and Solar Cells 91 (2007) 954.
[25] N. Blouin, A. Michaud, D. Gendron, S. Wakim, E. Blair, R. Neagu-Plesu, M. Belleêete, G. Durocher, Y. Tao, M. Leclerc, Journal of the American Chemical Society 130 (2008) 732.
[26] E. Zhou, J. Cong, K. Tajima, C. Yang, K. Hashimoto, Journal of Physical Chemistry C 116 (2012) 2608.
[27] T.-Y. Chu, J. Lu, S. Beaupre, Y. Zhang, J.-R. Pouliot, S. Wakim, J. Zhou, M. Leclerc, Z. Li, J. Ding, Y. Tao, Journal of the American Chemical Society 133 (2011) 4250.
[28] C.M. Amb, S. Chen, K.R. Graham, J. Subbiah, C.E. Small, F. So, J.R. Reynolds, Journal of the American Chemical Society 133 (2011) 10062.
[29] J.-Y. Lee, M.-H. Choi, H.-J. Song, D.-K. Moon, Journal of Polymer Science Part A: Polymer Chemistry 48 (2010) 3942.
[30] Y. Zhang, J. Zou, H.-L. Yip, K.-S. Chen, D.F. Zeigler, Y. Sun, A.K.-Y. Jen, Chemistry of Materials 23 (2011) 2289.
[31] A. Najari, S. Beaupré, P. Berrouard, Y. Zou, J.-R. Pouliot, C. Lepage-Pérusse, M. Leclerc, Advanced Functional Materials 21 (2011) 718.
[32] J. Li, A.C. Grimsdale, Chemical Society Reviews 39 (2010) 2399.
[33] G.-Y. Chen, Y.-H. Cheng, Y.-J. Chou, M.-S. Su, C.-M. Chen, K.-H. Wei, Chemical Communications 47 (2011) 5064.
[34] A. Najari, P. Berrouard, C. Ottone, M. Boivin, Y. Zou, D. Gendron, W.-O. Caron, P. Legros, C.N. Allen, S. Sadki, M. Leclerc, Macromolecules 45 (2012) 1833.
[35] Z. Lin, J. Bjorgaard, A.G. Yavuz, A. Iyer, M.E. Köse, RSC Advances 2 (2012) 642.
[36] H. Zhou, L. Yang, S. Stoneking, W. You, Applied Materials and Interfaces 2 (2010) 1377.
[37] J.Y. Lee, K.W. Song, J.R. Ku, T.H. Sung, D.K. Moon, Solar Energy Materials and Solar Cells 95 (2011) 3377.
[38] N. Blouin, A. Michaud, D. Gendron, S. Wakim, E. Blair, R. Neagu-Plesu, M. Belletête, G. Durocher, Y. Tao, M. Leclerc, Journal of the American Chemical Society 130 (2008) 732.
[39] S. Beaupréê, M. Belletête, G. Durocher, M. Leclerc, Macromolecular Theory and Simulations 20 (2011) 13.
[40] J.Y. Lee, S.M. Lee, K.W. Song, D.K. Moon, European Polymer Journal 48 (2012) 532.
[41] Y. Yao, C. Shi, G. Li, V. Shrotriya, Q. Pei, Y. Yang, Applied Physics Letters 89 (2006), 153507–53507-3.